IEEE Access
Multidisciplinary | Rapid Review | Open Access Journal

Received January 27, 2020, accepted February 24, 2020, date of publication March 2, 2020, date of current version March 13, 2020.

Digital Object Identifier 10.1109/ACCESS.2020.2977371

Accurate DOA Estimation With Adjacent Angle Power Difference for Indoor Localization

XIN ZHOU[1], LIANG CHEN[1,2], JUN YAN[3], AND RUIZHI CHEN[1,2]

[1]State Key Laboratory of Information Engineering in Surveying, Mapping, and Remote Sensing, Wuhan University, Wuhan 430079, China
[2]Collaborative Innovation Center of Geospatial Technology, Wuhan University, Wuhan 430079, China
[3]College of Telecommunications and Information Engineering, Nanjing University of Posts and Telecommunications, Nanjing 210003, China

Corresponding author: Liang Chen (l.chen@whu.edu.cn)

This work was supported in part by the National Thirteenth Five-Year Key R & D Plan Project of China, "New Urbanization Construction and Management Spatial Information Comprehensive Service and Application Demonstration," (project number: 2018YFB0505400), 2018-2022, participation, and in part by the Hubei Provincial Natural Science Foundation plan innovative group project "New mechanism for intelligent environment perception enhanced high precision indoor navigation and positioning," project number: 2018CFA007.

ABSTRACT Indoor localization with high accuracy plays a key role in the field of Internet of Things in 5th-Generation (5G) era. With the introduction of Multiple Input Multiple Output (MIMO) technology in 5G, the direction-of-arrival (DOA) method is highly feasible in indoor localization. However, the direction of arrival is susceptible to complex indoor environment. To improve the accuracy and stability of DOA estimation, an adjacent angle power difference (AAPD) method is proposed based on Orthogonal Matching Pursuit (OMP). This method uses OMP to obtain an initial estimate of the direction, and then, adjusts the estimation by calculating the difference power of adjacent points at initial value point to get the fractional DOA. In the scenario of continuous movement, beamforming is further applied, which reduces the amount of calculation. Both simulation and experimental results show that the proposed method can achieve high accuracy and eliminate the error jitter. Compared with the classical Multiple Signal Classification (MUSIC) method for DOA estimation, the proposed method can increase accuracy by 46% under the condition of low SNR (Signal-to-Noise Ratio). The probability that the measurement error does not exceed 5° in the actual movement tests is 97.5%.

INDEX TERMS Direction of arrival, 5G, orthogonal frequency division multiplexing, orthogonal matching pursuit, adjacent angle power difference, indoor localization.

I. INTRODUCTION

Information of location is becoming increasingly important in our daily life [1], and the location-based services (LBS) have been indispensable in medical, military, traffic, and so on [2]. Indoor localization with high accuracy has play pivotal roles in location-based services. The Global Navigation Satellite System (GNSS) outdoors cannot be effectively applied to indoor localization because the signals are too weak to be able to penetrate indoors [3]. Therefore, signal of opportunity (SOP) based and sensors-based techniques have been developed for indoor environments [4], such as WIFI [5], UWB [6], Bluetooth [7], RFID [8], geomagnetism [9], and ultrasound [10]. At present, with the development of wireless communication technology, 5th generation mobile networks (5G) have been closely related to daily life [11], [12]. In order to achieve low cost and widely available indoor localization without additional hardware, 5G wireless signal-based localization is gradually becoming ubiquitous.

The performance goals of 5G are to meet low latency, high transmission rates, and increase system capacity [13]. To achieve these goals, 5G systems introduce some innovative technologies, including Orthogonal Frequency Division Multiplexing (OFDM) technology and Multiple Input Multiple Output (MIMO) technology. The OFDM technology can be extended to large bandwidth applications, and has high spectral efficiency and low complexity [14]. The MIMO technology has become a research hotspot in the field of wireless technology, and the principle of MIMO is shown in Fig. 1. After the space time coded, the signal is divided into N_{trans} transmit sub-streams and transmitted through N_{trans} antennas. The signal is received through an array of M_{rec} antennas, and is subjected to space time decoding. By using multiple antennas on the transmitter and receiver, MIMO technology can effectively utilize spatial multiplexing techniques to improve communication quality and increase system transmission capacity. As the number of antennas increases, it can provide

The associate editor coordinating the review of this manuscript and approving it for publication was Hasan S. Mir.

This work is licensed under a Creative Commons Attribution 4.0 License. For more information, see http://creativecommons.org/licenses/by/4.0/

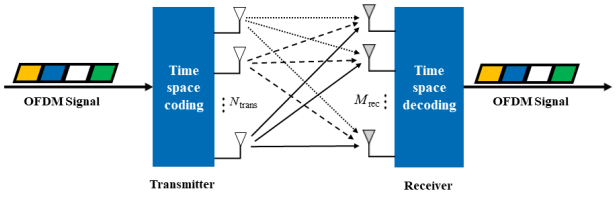

FIGURE 1. MIMO principle diagram.

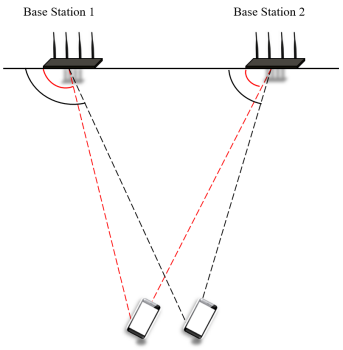

FIGURE 2. Positioning with DOA.

better diversity gain, thereby enhancing the reliability of the transmission link and increasing the transmission rate [15].

With the introduction of MIMO technology in 5G systems, antenna arrays-based direction-of-arrival (DOA) [16] method has more advantages and becomes increasingly important in the field of indoor localization. The localization principle of DOA method is shown in Fig. 2.

Wireless signal-based Indoor localization methods mainly include fingerprint [17], DOA, time-of-arrival (TOA) [18], [19], and time-difference-of-arrival (TDOA) [20]. Fingerprint method requires a huge workload to establish the fingerprint database and update the fingerprint database offline, so it is difficult for fingerprint method to adapt to the large changes in the field environment [21]. Compared with fingerprint, the implementation cost of DOA is lower, because this method can avoid the workload caused by establishing and updating the fingerprint database. TOA requires strict time synchronization between the transmitter and receiver, which increases the complexity of the system [22]. TDOA uses the propagation time difference between the receivers and it loses information about the signal departure time [20]. Compared with TOA and TDOA, DOA does not requires rigorous time information, therefore, it can reduce system complexity. One key challenge for DOA method is the strong multipath reflections in the indoor environment, and only the direct path is pointing to the true location of the target [23].

In the DOA estimation methods, the spatial spectrum estimation is a high-resolution method, and widely used in the design of smart antenna, mainly including Multiple Signal Classification (MUSIC), Estimating Signal Parameters via Rotational Invariance Techniques (ESPRIT), and Root-based Multiple Signal Classification (ROOT-MUSIC). MUSIC has proven to be the classic algorithm in DOA, and it has broader application prospects than ESPRIT [24]. Orthogonal Matching Pursuit (OMP) achieves more stable estimation results and achieves lower computational complexity than MUSIC [25]. However, the estimation accuracy of both methods depends on the constructed spatial grid matrix. In order to achieve high precision, it is necessary to divide a fine spatial grid, which will increase the amount of calculation. In addition, during the continuous movement process, the amount of repetitive calculation is large, and it is easy to produce error estimation due to the influence of multipaths. In this paper, considering the problem of improving the measurement accuracy and reducing the computational complexity, we proposed the adjacent angle power difference (AAPD) method. The main idea of this method is to use OMP to obtain an initial estimation of DOA, and then adjusts the estimation by calculating the difference power of adjacent points at initial value point to obtain a higher-precision estimation of DOA. In the continuous movement process, the proposed method only needs to perform once coarse grid search which effectively reduce the amount of repetitive calculation. Moreover, by using the estimation result of previous position as the starting point for the calculation of next position can effectively reduce the probability of error jitter occurring.

This paper is organized as follows: Section II briefly describes the OFDM signal mathematical model. Section III describes the high-precision DOA estimation AAPD method proposed in detail, and analyzes the performance of this method. Section IV describes the simulation test, we compared the MUSIC, ESPRIT, and OMP with our proposed method. Field tests are described to verify the effectiveness of the proposed method, and the results are discussed in Section V. Finally, Section VI concludes the paper and points out the future work.

II. THE SIGNAL MATHEMATICAL MODEL

An OFDM signal is a multi-carriers narrowband modulated signal that is effective for frequency selective fading [26]. Combined with MIMO technology, signal transmission performance in indoor environment can be improved [27]. Therefore, using OFDM signals to study DOA estimation based on antenna arrays will play a crucial role in indoor localization.

OFDM allocates the transmission band to N narrower continuous sub-bands (carriers) that are orthogonal to each other. Through orthogonality between subcarriers, the OFDM signals achieve robustness on frequency selective fading channels and eliminate adjacent subcarrier interference so that OFDM can make full use of the limited bandwidth. Fig. 3 shows the modulation of the OFDM signals with orthogonal subcarriers, and waveform data generated by different frequencies are superimposed in the time domain.

The signal generation process is shown in Fig. 4, the OFDM signal is modulated as complex data symbols by inverse discrete Fourier transform (IDFT), inserts a cyclic

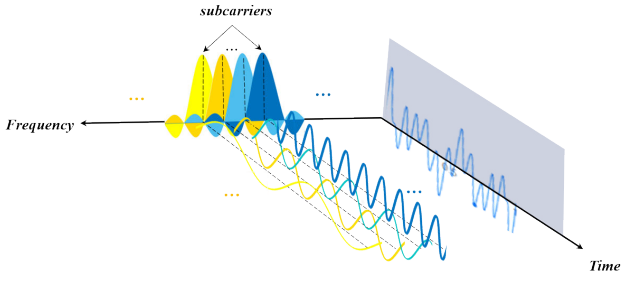

FIGURE 3. OFDM principle diagram.

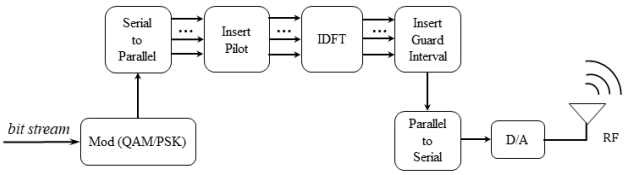

FIGURE 4. OFDM signal generation process.

prefix, and then performs parallel-to-serial conversion to generate a time domain signal for transmission.

It is assumed that the total number of subcarriers in the OFDM system is N, and the time domain signal is obtained after the IFFT operation on originally transmitted symbols. The baseband signal after sampling can be expressed as:

$$s(w) = \frac{1}{\sqrt{N}} \sum_{n=1}^{N} c_n \cdot \exp\left\{\frac{\mathrm{j} \cdot 2\pi wn}{N}\right\} \quad w = 0, \ldots, N-1 \tag{1}$$

where c_n is the data modulated on the n-th subcarrier.

Taking the OFDM signal as the incident signal and considering the receiving antenna array model as a uniform linear array (ULA), it is assumed that the number of antennas is M and the spacing between the antennas is d. We use the first antenna as the reference, and use the far-field signals received by linear antenna array as the incident signals with the number of m ($m < M$). At time k, signals received by the receiver can be represented as the vector:

$$\boldsymbol{x}(k) = [x_1(k), \ \ldots \ , x_M(k)]^T \tag{2}$$

whereas the m far-field signals can be expressed by:

$$\boldsymbol{s}(k) = [s_1(k), \ \ldots \ , s_m(k)]^T \tag{3}$$

The angles of the incident signals are defined as $\{\varphi_i \,|i = 1, \cdots, m\}$, the array steering vector corresponding to the incident signal is:

$$\begin{aligned} \boldsymbol{a}(\varphi_i) &= \left[e^{-jw_0\tau_{1i}} e^{-jw_0\tau_{2i}} \ \ldots \ \ e^{-jw_0\tau_{Mi}}\right]^T \\ \tau_{pi} &= \frac{1}{c} \cdot (p-1) \cdot d\cos(\varphi_i) \quad p = 1, \ldots, M \end{aligned} \tag{4}$$

where $w_0 = 2\pi c/\lambda$, λ is the signal wavelength and c is the propagation speed of electromagnetic waves in space. The spacing d between the antennas is equal to half of the wavelength. So, for m far-field incident signals, we can get a steering array is $\mathbf{A} = [\boldsymbol{a}(\varphi_1), \ldots, \boldsymbol{a}(\varphi_m)]$. By considering the added white Gaussian noise (AWGN) in the receiver, the signal received at time k can be modeled by:

$$\boldsymbol{x}(k) = \mathbf{A} \cdot \boldsymbol{s}(k) + \boldsymbol{v}(k) \tag{5}$$

where $\boldsymbol{v}(k)$ is the noise vector at time k. After N snapshots, we can get the received data of the entire array which is $\mathbf{Y}_N = \{\boldsymbol{x}(n) \,|n = 1, \ldots, N\}$, where $\mathbf{Y}_N$ is a $M \times N$ array matrix.

III. DOA ESTIMATION FOR INDOOR LOCALIZATION

The spatial spectrum estimation method of DOA estimation mainly including MUSIC, ESPRIT, and ROOT-MUSIC. MUSIC provides accurate detection of the angle of arrival than that of ESPRIT [28]. ROOT-MUSIC and MUSIC both use the orthogonality of the signal subspace and the noise subspace, but in ROOT-MUSIC, it uses analytical solutions to the covariance matrix instead of spectral peak search. ROOT-MUSIC's performance is better than ESPRIT at low SNR (Signal-to-Noise Ratio) [29], and is slightly better than MUSIC. However, due to the use of analytical solutions, the computational complexity of ROOT-MUSIC is higher than MUSIC [30].

Furthermore, the well-known greedy algorithm is OMP, which has proven to be viable in DOA estimation and provides a reasonable trade-off between computational complexity and accuracy [31], [32]. In this section, we describe in detail the proposed AAPD method, which includes DOA initial value acquisition and high-precision estimation.

A. THE DOA INITIAL VALUE ACQUISITION

In the DOA initial value acquisition, MUSIC and OMP are considered. MUSIC is a classical spatial domain method that performs beamforming by utilizing the orthogonality between the noise subspace and the steering vector representing the signal direction, and then performs spectral peak search. In order to obtain the value of DOA estimation, MUSIC method needs to solve the covariance matrix $\mathbf{R}_{XX}$ and perform eigenvalue decomposition to obtain the noise subspace as $\mathbf{E}_{\mathrm{n}}$. According to the orthogonality, the length of the vector obtained by multiplying the steering vector of the space signal with the noise subspace can be recorded as:

$$L_{\mathrm{m}} = \left\| \mathbf{E}_{\mathrm{n}}^H \boldsymbol{a}(\theta_i) \right\| \tag{6}$$

where $\boldsymbol{a}(\cdot)$ is defined in (4), and $\{\theta_i \,|i = 1, \cdots, N_s\}$ denotes the angles of space signals. N_s is the number of grids divided by the space $[0, \pi]$. The divisional fineness of the spatial grid determines the estimation accuracy of the DOA, and Fig. 5 shows the division of the spatial grid. The squared value of L_{m} is infinitely close to 0 when θ_i is equal to the angle of incident signal. The search spectrum of the MUSIC is defined as:

$$SP(\theta_i) = \frac{1}{||L_{\mathrm{m}}||^2} = \frac{1}{\boldsymbol{a}^H(\theta_i) \cdot \mathbf{E}_{\mathrm{n}} \cdot \mathbf{E}_{\mathrm{n}}^H \cdot \boldsymbol{a}(\theta_i)} \quad i = 1, \ldots, N_s \tag{7}$$

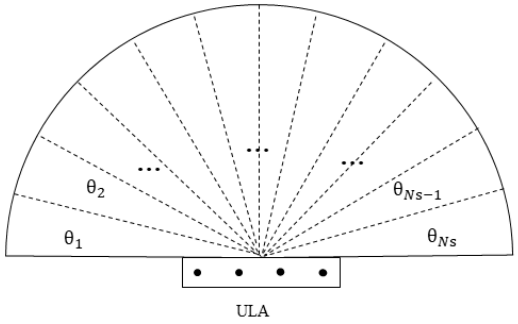

FIGURE 5. The division of the spatial grid.

The performance of MUSIC is good when the SNR is enough, and the estimation accuracy increases with the sampling snapshots. However, this method will increase the amount of computation for covariance solving of the received signal, and the MUSIC has a very high requirement for incident signals. The premise of applying this method is that incident signals must be uncorrelated. When the number of sensors is same as the size of the snapshot N_s, the standard statistical analysis of MUSIC is uncorrelated, because MUSIC mainly relies on the sample correlation matrix $\mathbf{R}_{XX}$ of the observation [33] which will affects the estimation accuracy in the case of less data or few antennas.

In order to improve the accuracy of DOA estimation and reduce the computational complexity in the case of low sampling data volume, OMP method is used in this paper. The OMP exploits the sparseness of the spatial domain of the incident signal, and estimates the angle of arrival by directly matching the received signal. The results in [34] shows that the OMP method is a better candidate for the DOA estimation, and the next chapter will prove that OMP has better performance than MUSIC.

In OMP, we assume that the sensing matrix is $\mathbf{H}$, and the number of sampling snapshots is N, we have M array antennas and m far-field signals. We already know that the received data is $\mathbf{Y}_N$. The sensing matrix represents the sparseness of the signal. The direction of arrival of the signal is a small part of the space $[0, \pi]$, so the direction of arrival of the incident signal is sparse throughout the space. The sensing matrix can be defined as:

$$\mathbf{H} = \begin{bmatrix} \boldsymbol{a}(\theta_1) & \boldsymbol{a}(\theta_2) & \cdots & \boldsymbol{a}(\theta_{N_s}) \end{bmatrix} \tag{8}$$

where $\boldsymbol{a}(\cdot)$ is defined in (4) and N_s is the number of grids divided by the space $[0, \pi]$. Then, we obtained the matrix $\mathbf{P}$ through match tracking. Here it is assumed that the initial value of the residual is $\mathbf{V}_N = \mathbf{Y}_N$, the index set $\Upsilon = \emptyset$, the most relevant column is stored at $\mathbf{A}_t$, and the matrix $\mathbf{P}$ is:

$$\mathbf{P} = \mathbf{H}^T \cdot \mathbf{V}_N = \begin{bmatrix} \boldsymbol{P}_1 & \boldsymbol{P}_2 & \cdots & \boldsymbol{P}_{N_s} \end{bmatrix}^T \tag{9}$$

where $\mathbf{P}$ is a $N_s \times N$ matrix, each row $\boldsymbol{P}_i$ of the $\mathbf{P}$ corresponds to each sparse point of the $\mathbf{H}$ matrix, and it represents the matching correlation value of the corresponding sparse point. In order to obtain a unique match value for each sparse point,

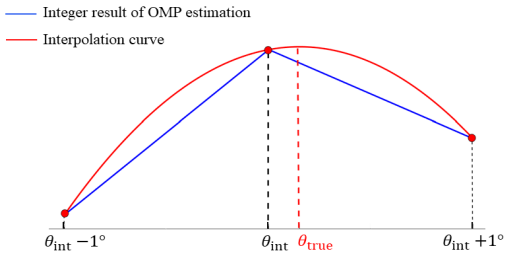

FIGURE 6. Integer value of DOA after OMP is deviate from the true value.

the $\mathbf{P}$ matrix is processed by the 2-Norm, and we select the largest value:

$$ind = \arg\max_i \left\{ \|\mathbf{p}_i\|_2 \right\} \tag{10}$$

where ind is stored in Υ, and corresponds to the column in the $\mathbf{H}$ matrix. The most relevant column is selected and stored in $\mathbf{A}_t$. Next, we use the least squares to get the new residual value:

$$\mathbf{X}_N = \left(\mathbf{A}_t^H \mathbf{A}_t \right)^{-1} \cdot \mathbf{A}_t^H \cdot \mathbf{V}_N \tag{11}$$

$$\mathbf{V}_N = \mathbf{Y}_N - \mathbf{A}_t \cdot \mathbf{X}_N \tag{12}$$

This obtained residual value $\mathbf{V}_N$ in (12) is then iteratively updated into (11) until m indexes corresponding to the m far-field signals are found, and the DOA estimation is obtained by considering the correspondence between the index and the space angle.

The advantage of the OMP is that, it does not require the covariance decomposition and thus, it is not sensitive to noise, which can achieve the estimation of the angle of arrival in low SNR. However, in each iteration, OMP requires an angular search in the entire spatial domain, which costs high computational complexity, especially in the case of high-precision DOA estimate is required. In this work, in order to further improve the accuracy of DOA and reduce the computational complexity, the AAPD method is used to obtain high-precision DOA estimation. Moreover, in order to reduce the redundant computation in the continuous movement process, the beamforming is introduced.

B. HIGH-PRECISION DOA ESTIMATION

After OMP, we get the integer value of DOA, but in most cases, the result is biased from the true value. As seen from Fig. 6, we suppose the initial value of DOA is θ_{int} and the true value is θ_{true}, the OMP result can be corrected by spline interpolation to obtain the fractional value of DOA.

Therefore, we proposed an AAPD method based on correlation function, and the reliability of the correlation function is verified in the algorithm analysis of this chapter. After obtaining the initial value of DOA by OMP, the AAPD method first needs to determine the region in which the peak falls. According to the principle in Fig. 7, we can get the region by comparing the power difference values R_l, R_r which are corresponding to the θ_{int}'s left and right adjacent points

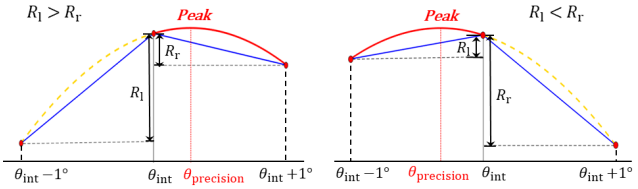

FIGURE 7. Determining the region where the peak is located.

respectively. Three red data points are corresponding to the integer value θ_{int} of DOA and its adjacent integer angles θ_l, and θ_r. The power values of these points are calculated by:

$$\begin{cases} r_\Sigma(\theta_{int}) = \left\| \boldsymbol{a}^H(\theta_{int}) \cdot \mathbf{Y}_N \right\|_2 \\ r_\Sigma(\theta_l) = \left\| \boldsymbol{a}^H(\theta_{int}-1) \cdot \mathbf{Y}_N \right\|_2 \\ r_\Sigma(\theta_r) = \left\| \boldsymbol{a}^H(\theta_{int}+1) \cdot \mathbf{Y}_N \right\|_2 \end{cases} \tag{13}$$

where $\mathbf{Y}_N$ is a $M \times N$ array matrix of receiving data. The range where the peak falls is determined by the power difference values R_l, R_r:

$$\begin{cases} R_l = |r_\Sigma(\theta_{int}) - r_\Sigma(\theta_l)| \\ R_r = |r_\Sigma(\theta_{int}) - r_\Sigma(\theta_r)| \end{cases} \tag{14}$$

The selected region is shown by the red curve in Fig. 7, which can be defined as D_θ. If $R_l > R_r$, the selected region is $D_\theta \triangleq [\theta_{int},\ \theta_{int}+1°]$. If $R_l < R_r$, the selected region is $D_\theta \triangleq [\theta_{int}-1°,\ \theta_{int}]$. We suppose the resolution is $\Delta\theta$, the selected region D_θ can be divided into n grid points which corresponding to different fractional angles, and the selected region can be recorded as:

$$D_\theta \triangleq \begin{cases} [\theta_{int}-1, \theta_{int}-1+\Delta\theta, \cdots, \theta_{int}] & R_l < R_r \\ [\theta_{int},\ \theta_{int}+\Delta\theta,\ \cdots,\ \theta_{int}+1] & R_l > R_r \end{cases} \tag{15}$$

where $\theta_i \in D_\theta (i = 1, 2, \cdots, n)$. and then, the correlation function results of the left and right adjacent points of each point in θ_i are solved. Thus, the power difference between the adjacent points is obtained by:

$$\Delta r_{power}(\theta_i) = \left\| \boldsymbol{a}^H(\theta_i - \Delta\theta) \cdot \mathbf{Y}_N \right\|_2 - \left\| \boldsymbol{a}^H(\theta_i + \Delta\theta) \cdot \mathbf{Y}_N \right\|_2 \tag{16}$$

As shown in Fig. 8, $\Delta\theta$ is the resolution we selected. By searching for the minimum value of the results in (16), we obtained the high accuracy value $\theta_{precision}$ of doa which corresponding to the minimum value, and it is calculated as follows:

$$\theta_{precision} = \arg\min_{\theta_i} \left| \Delta r_{power}(\theta_i) \right| \tag{17}$$

In this work, the AAPD method can get the fractional value of DOA. The process of this method can be summarized as,

- get the integer value of DOA by OMP method, and then take out the left and right adjacent points, and determine the range where fractional value of DOA falls.
- subdivide the selected range.

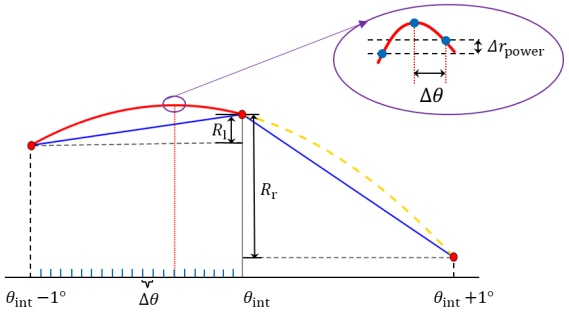

FIGURE 8. Schematic diagram of the AAPD method.

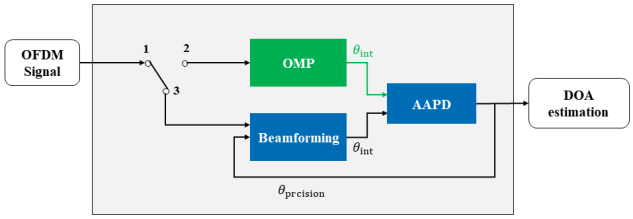

FIGURE 9. Principle of the high-precision arrival angle estimation.

- calculate the power difference between the adjacent points at each point in the selected range after subdivided to represent the search value of that point.
- find the minimum search value to get the point, which can represent the fractional value of DOA.

C. THE CONTINUOUS MOVEMENT PROCESSES

Considering the process of continuous movement, the DOA of the current location is related to the DOA of the previous location, so we set a symmetry region. the angle obtained from the previous position is set to the center of the symmetrical region, and the integer value of DOA estimation is performed by beamforming at the current position, and then high-precision estimation is performed. Beamforming utilizes correlation function which modeled as:

$$r_\Sigma(\theta_i) = \left\| \boldsymbol{a}^H(\theta_i) \cdot \mathbf{Y}_N \right\|_2 \tag{18}$$

where θ_i is in the symmetrical region, $\mathbf{Y}_N$ is the receiving data. The framework of the entire process is depicted in Fig. 9 where the switch 1 is sequentially switched to the position 2, and 3 to do the first estimation, and the others estimation.

The symmetry region determined by the actual situation. Here we did the analysis, as shown in Fig. 10. We know that people have a maximum step size when they walk. Referring to the research results in [35], the maximum speed of human movement is 2.53 m/s considering the gender and age. The experimental operation efficiency is tested in this study, and the average running time is 53 ms. In order to facilitate the calculation and consider fault tolerance, we take the running time of each algorithm as 60 ms = 0.06 s, and the maximum speed of human movement is 3m/s, then the distance between each two estimated positions is 0.18 m. Fig. 10 shows that the

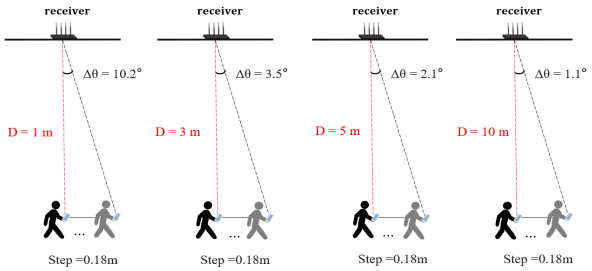

FIGURE 10. Step length analysis with different distance.

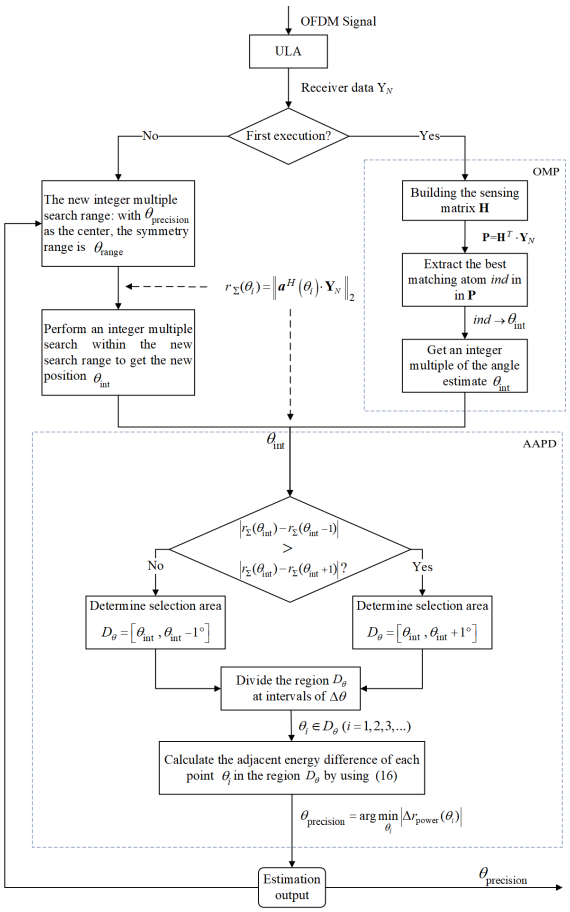

FIGURE 11. Framework for continuous movement method proposed.

angle of step movement decreases as the distance between the person and the receiving node increases. Considering the different case, we choose a symmetry range of $\theta_{\text{range}} = 30°$ which can include all step angles in movement, and then use θ_{range} as the beamforming range to obtain the integer value of DOA of the new position. Therefore, there is no need to build a sensing matrix again during the search process, and we choose beamforming technology to avoid complete spatial search which will save computation time and decrease the complexity. The entire framework for continuous movement process is shown in Fig. 11, and the entire proposed method is summarized as follows:

Algorithm 1 Adjacent Angle Power Difference

1. **Integer multiple angle acquisition:**
   if the new OFDM signals are received
   if the algorithm is executed for the first time **then**
   Divide the spatial angles to construct the sensing matrix **H**
   And then get integer value θ_{int} of DOA by OMP.
   else
   A beamforming area with a range of θ_{range} is established centered on $\theta_{\text{precision}}$
   And an integral multiple angle of the new position is estimated θ_{int}.
   end if
   end if
2. **Determine the ideal region (selection region):**
   Compare the power values of $\theta_{\text{int}} - \varepsilon \rightarrow R_{\text{l}}$ and $\theta_{\text{int}} + \varepsilon \rightarrow R_{\text{r}}$, where $\varepsilon = 1°$
   if $R_l > R_r$ **then**
   The ideal region to choose is $D_\theta = [\theta_{\text{int}},\ \theta_{\text{int}} + \varepsilon]$.
   else
   The ideal region to choose is $D_\theta = [\theta_{\text{int}} - \varepsilon,\ \theta_{int}]$.
   end if
   Divide the ideal area D_θ by $\Delta\theta$.
3. **Adjacent point difference:**
   After division, all points in the ideal area are recorded as $\theta_i \in D_\theta\ (i = 1, 2, 3, \ldots)$,
   and calculate the power difference between adjacent points of $\Delta r_{\text{power}}(\theta_i)$,
   return $\theta_{\text{precision}} = \theta_i \longleftarrow \arg\min_{\theta_i} \left|\Delta r_{\text{power}}(\theta_i)\right|$ as the result.
3. **Re-estimate integer multiple angle and output:**
   if the DOA is estimated to end **then**
   stop.
   else
   output $\theta_{\text{precision}}$
   and reset $\theta_{\text{int}} = \theta_{\text{precision}}$ then go to Phase 1.
   end if

D. ALGORITHM ANALYSIS

1) FEASIBILITY ANALYSIS

To further verify the feasibility of the proposed method, we analyzed the performance of the correlation function in (18). Without the noise, the signal $\boldsymbol{s}_N$ can be defined as:

$$\boldsymbol{s}_N = [s(1) \quad s(2) \quad \ldots \quad s(N)] \tag{19}$$

where $s(i)$ is defined in (1), and $i = 1, \ldots, N$. It is assumed that the actual incident angle of the signal is β, then β is substituted into (4) to obtain a phase difference parameter for each antenna of the receiving array. The received signal can be expressed as:

$$\mathbf{Y}_N = \boldsymbol{a}(\beta) \cdot \boldsymbol{s}_N \tag{20}$$

Assuming the angle of the spatial search is α and $\alpha \in [0\,,\ 180°]$, the representation of the correlation function

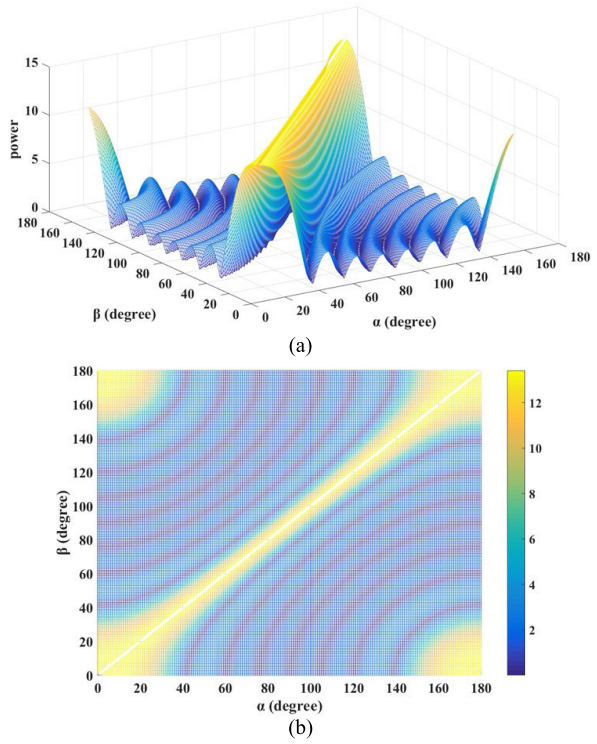

FIGURE 12. The relationship between the correlation function value and α, β. (a) The 3D view of the relationship. (b) The top view of the relationship.

can be expressed as:

$$CF(\alpha,\beta) = \frac{1}{N}\sum \boldsymbol{a}^*(\alpha)\cdot \mathbf{Y}_N = \frac{1}{N}\sum_{i=1}^{N} \boldsymbol{a}^*(\alpha)\cdot \boldsymbol{a}(\beta)\cdot s(i) \quad (21)$$

where $\boldsymbol{a}^*(\alpha)\cdot\boldsymbol{a}(\beta)$ is the sum of the Geometric Progression, thus, (21) is equal to:

$$CF(\alpha,\beta) = \frac{1}{N}\cdot\frac{1-e^{j\frac{2\pi d}{\lambda}M(\cos(\alpha)-\cos(\beta))}}{1-e^{j\frac{2\pi d}{\lambda}(\cos(\alpha)-\cos(\beta))}}\cdot \boldsymbol{s}_N \quad (22)$$

Fig. 12 provides a diagram representation of equation (22). The value of $CF(\alpha,\beta)$ can be obtained by the transformation of α, β. It can be seen that when α and β are consistent, $CF(\alpha,\beta)$ can obtain the maximum value. This proves the feasibility of the method proposed.

2) COMPLEXITY ANALYSIS

Considering that it is necessary to perform DOA estimation of different positions many times in the case of actual movement, we assume that the DOA estimation is performed n times. The number of sampling data is N, the number of antennas in receiver is M, and the fractional angle resolution is $\Delta\theta = 0.1$. The operation complexity of the three methods are as follows:

$$\mathbf{O}(MUSIC) = \mathbf{O}((180/\Delta\theta^* M^* N + M^* N^* M)^n)$$
$$\mathbf{O}(OMP) = \mathbf{O}((180/\Delta\theta^* M^* N)^n)$$

TABLE 1. Simulation parameters.

Parameters	Value
FFT Size(snapshot)	512
CP ratio	1/4
sampling rate	20M
center frequency	2.4GHz
number of antennas	4

$$\mathbf{O}(OMP + AAPD) = \mathbf{O}((180^* M^* N) + (30^* M^* N + 20^* M^* N)^{n-1}) \quad (23)$$

According to the increase of the number n, the complexity of the three methods are compared in:

$$\mathbf{O}(OMP) \ll \mathbf{O}(MUSIC)$$
$$\mathbf{O}(OMP + AAPD) \ll \mathbf{O}(OMP) \quad (24)$$

In (23), If the OMP method is used directly to obtain the same angle estimation resolution as the proposed method, the number of operations of the algorithm in continuous movement process is greatly increased which will causes greater system overhead. In (24), the proposed OMP + AAPD method can greatly reduce the amount of computation. In summary, the proposed method can improve the estimation accuracy of the OMP algorithm and greatly reduce the system overhead, which will play an important role in the indoor positioning of real-time mobile measurement.

IV. SIMULATION TESTS FOR DOA ESTIMATION

In this section, the performance of the proposed method was analyzed. Firstly, we analyzed the DOA estimation method by comparing OMP with MUSIC, ROOT-MUSIC, ESPRIT. Accuracy analysis based on root mean square error (RMSE) and we assumed that the number of antennas tested is M = 4, and the Monte Carlo experiments were performed by using the OFDM signals and the number of snapshots is 512. The simulation parameters used are listed in Table 1. Fig. 13 shows the performance of different methods with respect to SNR. As seen from the figure, the RMSE of both methods are decreased as SNR increased, and the OMP method performed better at the low SNR. At the same time, we know that OMP can avoid the covariance decomposition required by other methods, Thus OMP can effectively reduce the computational complexity. The consumption time is shown in Table 2. As seen from this analysis in Table 2 and Fig 13, the OMP method has a better performance than other methods, and the ROOT-MUSIC has a slightly better than the MUSIC in the low SNR, but the computation is more expensive.

Based on the advantages of OMP, we used OMP to get the integer value of DOA, and then used AAPD method to improve estimation accuracy. The interpolation method was taken as a reference. In order to show the estimation effect of the proposed method more clearly, we performed Monte

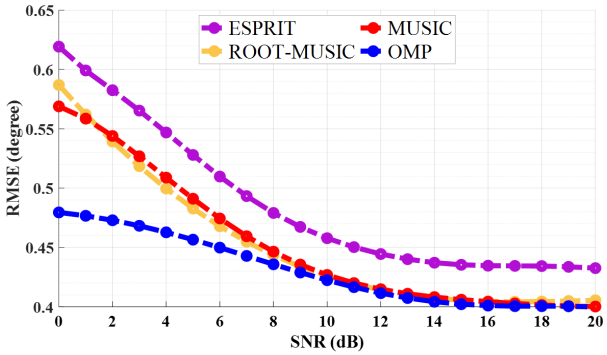

FIGURE 13. Comparison of the results of OMP and MUSIC, ESPRIT, ROOT - MUSIC with respect to SNR.

TABLE 2. Time consumption for different methods.

Methods	Average time consumption/ms
ESPRIT	116
ROOT-MUSIC	258
MUSIC	127
OMP	67
OMP + Interpolation	49
OMP + AAPD	45

Carlo experiments with the number of antennas in receiver is $M = 4$ and the number of snapshots is 512. The RMSE curve was drawn by using the SNR variation, as shown in the Fig. 14. It can be seen that the proposed method has improved in accuracy with the increasing of SNR than OMP. Moreover, the AAPD is more accurate than the interpolation method. Combining Fig. 13 and Fig. 14, we can get that the AAPD method proposed can increase accuracy by 46% compared with MUSIC under the condition of low SNR. On the other hand, as seen from Table 2, the time consumption of the proposed method is greatly reduced compared to the MUSIC and OMP. In consideration of the actual continuous movement, we conducted the following experiments. Based on the previous analysis, we chose a symmetry region of $\theta_{\text{range}} = 30°$ as the search region for the next position. When the starting position is set to 53.6°, a step moving angle of 0-15° is randomly generated, and 8 movements are continuously performed. The true values of the obtained position angles are 53.6°, 63.6°, 74.4°, 79.5°, 89.8°, 100°, 110 °, 112.8°. The total mean error of 8 positions was calculated at each time, and the Monte Carlo experiments were conducted. Then, using RMSE and CDF (Cumulative Distribution Function) to performance analysis. The RMSE estimation results are shown in Fig. 15. As seen from this analysis result, the proposed method in this paper can effectively reduce the measurement error. Under the continuous movement condition, the total mean error of 8 positions was calculated for each experiment, so the RMSE value is less than the RMSE of one position, but this does not affect the algorithm performance under the condition as the SNR changes. Moreover, we obtained the

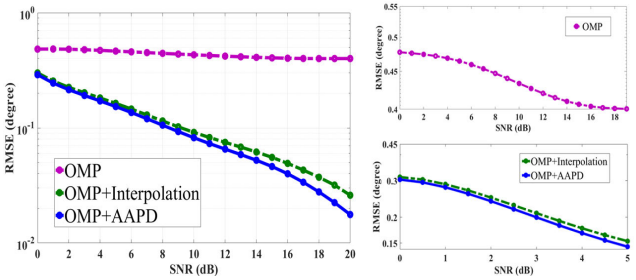

FIGURE 14. Comparison of the method proposed with the traditional OMP with respect to SNR.

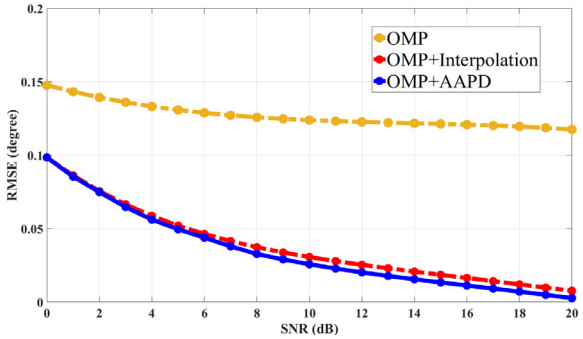

FIGURE 15. Comparison of calculation errors of multiple locations under the moving condition.

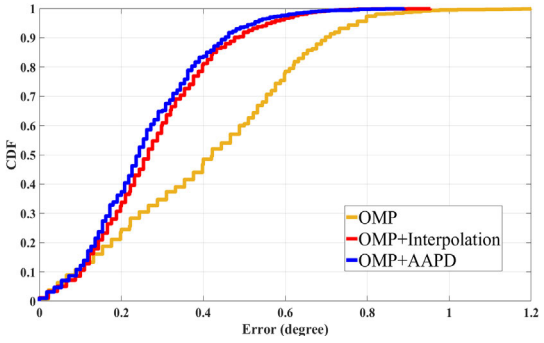

FIGURE 16. Comparison of calculation errors of multiple locations under the moving condition with CDF.

CDF results of the estimated error which as shown in Fig. 16. It can be seen that the probability of error greater than 0.5° is less than 10% in the proposed method, and which is approximately 60% in OMP. Therefore, the proposed method can effectively improve the estimation accuracy than both OMP and MUSIC.

V. EXPERIMENTS AND RESULTS IN INDOOR ENVIRONMENT

To verify the effectiveness of the proposed method, we tested in an indoor environment with a low height and complicated conditions such as glass, chairs, spotlights, and irregular walls and so on, as shown in Fig. 17. The test used a ULA of 4 antennas with the antennas spacing equal to half of the wavelength and the height of the receiving antenna array is

TABLE 3. Statistics of angle error of the proposed OMP + AAPD method.

Degree	Check points	Points with error < 1°	Detected accuracy	RMSE/degree
60°	399	332	83.21%	2.1486
90°	373	357	95.71%	1.7417
120°	699	628	89.84%	1.8379
Total	1471	1317	89.53%	1.9044

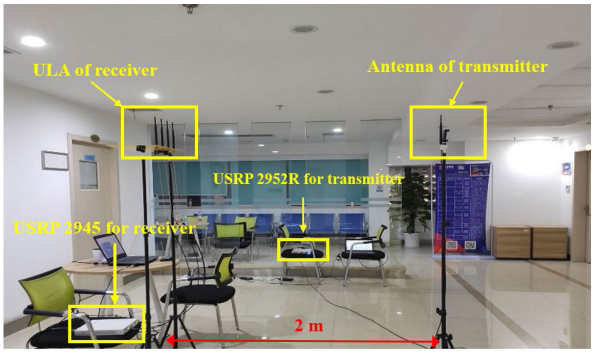

FIGURE 17. Testing scenario.

FIGURE 18. Testing bench.

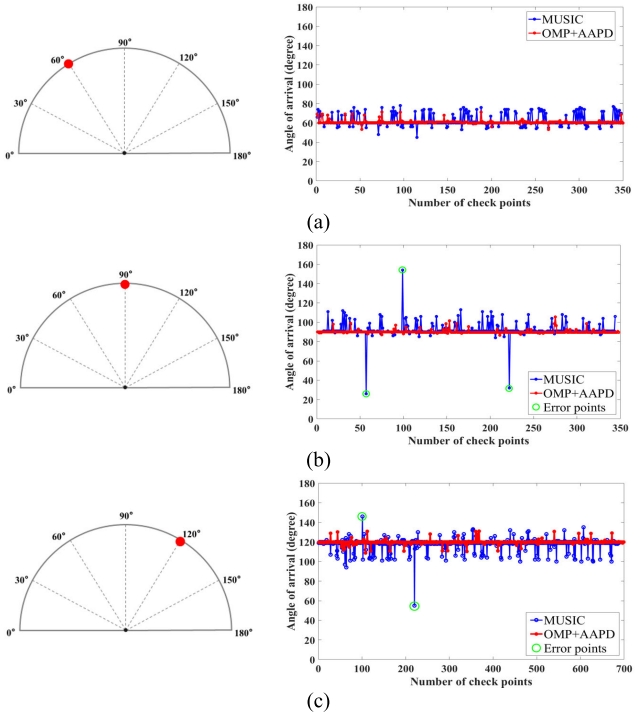

FIGURE 19. Angle measurement results of the proposed OMP + AAPD and MUSIC in static mode. (a) Static angle measurement result of 60°. (b) Static angle measurement result of 90°. (c) Static angle measurement result of 120°.

set to 1.8 m. The signals transmitted by the transmitter are OFDM signals in the 2.404GHz band, and the height of the transmitter end antenna is 1.8 m. The distance between the receiver and the transmitter measured by the range finder is 2 m. The signal transmitting platform used in this test is built by NI USRP-2952R and GNU Radio, and the receiving platform is built by NI USRP-2945 and LABVIEW. In the receiving platform, we can simultaneously perform MUSIC and the proposed method.

NI USRP [36] is a low-cost, flexible open source device for manufacturing software radio that can send and receive high-frequency signals. LABVIEW is a graphical data flow programming language which is ideal for designing and implementing communication algorithms. Both NI USRP hardware and LabVIEW software are flexible, powerful, and affordable. GNU Radio is a fully open source, highly modular flow chart software radio architecture platform that allows users to use these modules for signal processing, while supporting the development of basic modules. The components of the test bench are shown in Fig. 18. We used USRP-2945 which can receive signals between 10 MHz to 6 GHz with a maximum bandwidth of 80 MHz. The device has four unattached receive channels and shares a local oscillator for phase coherent operation, it is equipped with a Kintex-7 FPGA for LABVIEW FPGA module programming. The USRP-2952R for transmitting signals has an RF range of 40 MHz to 4.4 GHz, and a bandwidth up to 120 MHz. It is also equipped with a Kintex-7 FPGA.

The test was divided into static testing and continuous movement. On the established Software Defined Radio (SDR) platform, the performance comparison was performed by using the classical MUSIC method and the proposed method in this paper.

A. STATIC TESTS

In the static tests, we chose three points of 60°, 90°, 120°, and collected data of each point for 15s-30s.

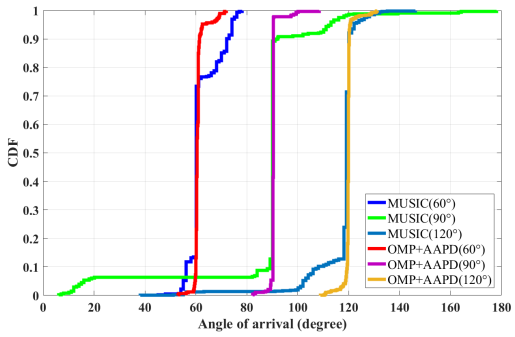

FIGURE 20. Comparison of measurement accuracy between OMP + AAPD and MUSIC at different angles.

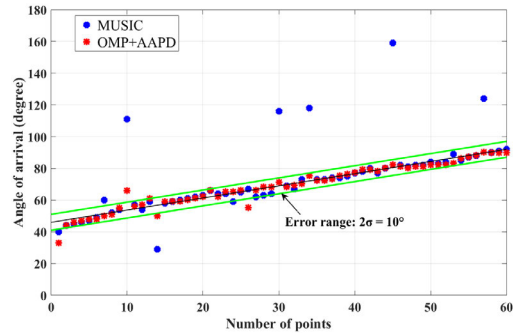

(a)

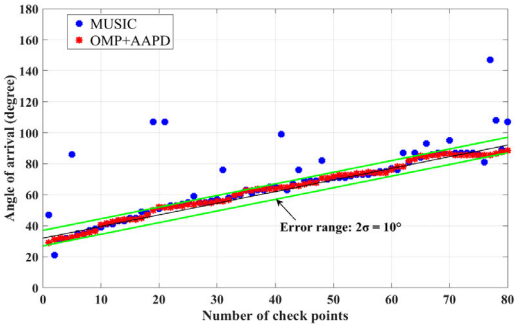

(b)

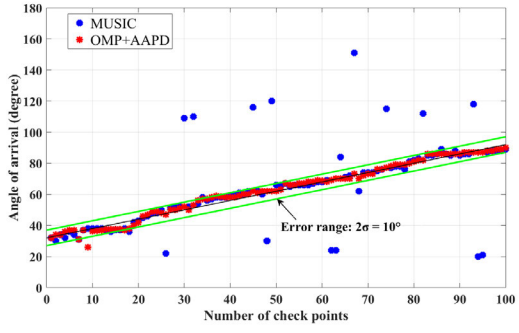

(c)

FIGURE 21. Comparison of measurement accuracy between MUSIC and OMP + AAPD at continuous movement. (a) test 1. (b) test 2. (c) test 3.

Fig. 19 provided the results of static data acquisition. The MUSIC had been distinguished from the proposed method in this Figure, and the point where the jitter is large was recorded as the estimated error point, which was circled. In the actual tests, both methods will fluctuate due to the influence of indoor multipath. It can be seen that MUSIC will have some error points, but the method proposed in this paper is stable in multiple test angles. As shown in Table 3, the accuracy of the method proposed was analyzed. The performance of the method was evaluated by calculating the number of points where the estimated error was less than 1°, and calculating the RMSE of the data collected at each test angle. Comparing with the real value, the number of points where the average estimated error less than 1° was 89.73%, and the average deviation of each estimation was 1.9044°, which proved the accuracy of the proposed method.

TABLE 4. Statistics of detected accuracy.

Test	Check points	Points with error < 5°	Detected accuracy
MUSIC	240	199	82.92%
OMP+AAPD	240	234	97.50%

To more intuitively show the advantages of the proposed method, we used the CDF to display the estimated point distribution of the MUSIC method and the proposed method at three measurement points. It can be seen from the Fig. 20 that at three test points, more than 90% of estimated points of the method proposed were concentrated near the true value, which was better than 60%-80% of MUSIC.

B. CONTINUOUS MOVEMENT PROCESSES

In the continuous movement tests, the distance between the receiving antenna array and the transmitting antenna is 2 m. During the test, the transmitting antenna moved at a constant speed and performed continuous sampling. Moreover, we observed the status of the dashboard which used to display DOA values of the receiver to confirm the test was performed correctly, as shown in Fig. 18. The test was repeated three times and the angle of arrival data were collected for analysis. The result was shown in Fig. 21. As the transmitting antenna approached a uniform speed, the measured angles should increase linearly. Using the average straight line marked in Fig. 21 as the reference line, the range of 5° above and below the reference line was marked as the range for performance analysis, and denoted it as the error range. Points that fallen within this range were considered ideal data. It can be seen that the classical MUSIC method generated more error jitter points during the motion, and the estimated error of the method proposed was basically kept within 5°, which had better performance.

For a more intuitive analysis, Table 4 summarized the number of ideal data points that fallen within the error range of the experimental data. The accuracy of MUSIC was 82.92%, and the method proposed can reach 97.50%, which was increased 14.58% than the accuracy of MUSIC. The test results shown that the method proposed can effectively eliminate the error jitter and improve the estimation accuracy.

VI. CONCLUSION

In this paper, a high precision DOA estimation method based on smart antennas was presented. The feasibility of the method was studied both from the perspective of theoretical analysis and practical experimental analysis.

Theoretical analysis shown that compared with OMP and MUSIC, this method can effectively reduce the computational complexity. In the simulation analysis, the proposed method can provide higher accuracy than OMP and MUSIC under the different SNR, and its accuracy was significantly improved with the increase of SNR. Moreover, the proposed AAPD method can increase accuracy by 46% compared with MUSIC under the condition of low SNR. Simulating the movement situation, we counted the total average error of 8 incremental angles, Monte Carlo experiments shown that the method proposed was 30% more likely to control the overall error within 0.5° than OMP.

In order to carry out the actual tests, we built the SDR angle measuring receiver based on NI USRP, and realized simultaneous angle measurements for the proposed method and MUSIC. The actual tests indicated that the method can eliminate the error jitter under continuous movement. In an indoor environment with multipaths, the mean error of static angle measurement was within 2°, and the probability that the measurement error does not exceed 5° in the actual movement tests is 97.5%. The analysis results shown that the proposed method can effectively improve the positioning accuracy and eliminate error jitter.

The multipath problems decrease the performance of DOA estimation. To reduce the negative impact caused by multipaths interference, and improve the adaptability of the AAPD method in the indoor environment, and further improve the accuracy of the angle measurements, effective solutions should be taken in the future.

REFERENCES

[1] L. Chen, O. Julien, E.-S. Lohan, G. Seco-Granados, and R. Chen, "Mobile geospatial computing systems for ubiquitous positioning," *Mobile Inf. Syst.*, vol. 2018, pp. 1–2, Jun. 2018.

[2] Z. Deng, Y. Yu, X. Yuan, N. Wan, and L. Yang, "Situation and development tendency of indoor positioning," *China Commun.*, vol. 10, no. 3, pp. 42–55, Mar. 2013.

[3] L. Chen, S. Thombre, K. Jarvinen, E. S. Lohan, A. Alen-Savikko, H. Leppakoski, M. Z. H. Bhuiyan, S. Bu-Pasha, G. N. Ferrara, S. Honkala, J. Lindqvist, L. Ruotsalainen, P. Korpisaari, and H. Kuusniemi, "Robustness, security and privacy in location-based services for future IoT: A survey," *IEEE Access*, vol. 5, pp. 8956–8977, 2017.

[4] F. Zafari, A. Gkelias, and K. K. Leung, "A survey of indoor localization systems and technologies," *IEEE Commun. Surveys Tuts.*, vol. 21, no. 3, pp. 2568–2599, 3rd Quart., 2019.

[5] H. Liu, H. Darabi, P. Banerjee, and J. Liu, "Survey of wireless indoor positioning techniques and systems," *IEEE Trans. Syst., Man, Cybern. C, Appl. Rev.*, vol. 37, no. 6, pp. 1067–1080, Nov. 2007.

[6] D. Dardari, A. Conti, U. Ferner, A. Giorgetti, and M. Z. Win, "Ranging with ultrawide bandwidth signals in multipath environments," *Proc. IEEE*, vol. 97, no. 2, pp. 404–426, Feb. 2009.

[7] L. Chen, L. Pei, H. Kuusniemi, Y. Chen, T. Kröger, and R. Chen, "Bayesian fusion for indoor positioning using Bluetooth fingerprints," *Wireless Pers. Commun.*, vol. 70, no. 4, pp. 1735–1745, 2013.

[8] N. Li and B. Becerik-Gerber, "Performance-based evaluation of RFID-based indoor location sensing solutions for the built environment," *Adv. Eng. Informat.*, vol. 25, no. 3, pp. 535–546, Aug. 2011.

[9] J. Chung, M. Donahoe, C. Schmandt, I.-J. Kim, P. Razavai, and M. Wiseman, "Indoor location sensing using geo-magnetism," in *Proc. 9th Int. Conf. Mobile Syst., Appl., Services (MobiSys)*, Bethesda, MD, USA, 2011, pp. 141–154.

[10] J. Qi and G.-P. Liu, "A robust high-accuracy ultrasound indoor positioning system based on a wireless sensor network," *Sensors*, vol. 17, no. 11, p. 2554, Nov. 2017.

[11] M. R. Palattella, M. Dohler, A. Grieco, G. Rizzo, J. Torsner, T. Engel, and L. Ladid, "Internet of Things in the 5G era: Enablers, architecture, and business models," *IEEE J. Sel. Areas Commun.*, vol. 34, no. 3, pp. 510–527, Mar. 2016.

[12] T. Mshvidobadze, "Evolution mobile wireless communication and LTE networks," in *Proc. 6th Int. Conf. Appl. Inf. Commun. Technol. (AICT)*, Tbilisi, Georgia, Oct. 2012, pp. 1–7.

[13] O. Oshin, M. Luka, and A. Atayero, "From 3GPP LTE to 5G: An evolution," in *Transactions on Engineering Technologies*. Singapore: Springer, pp. 485–502, Jun. 2016.

[14] M. Agiwal, A. Roy, and N. Saxena, "Next generation 5G wireless networks: A comprehensive survey," *IEEE Commun. Surveys Tuts.*, vol. 18, no. 3, pp. 1617–1655, 3rd Quart., 2016.

[15] O. Elijah, C. Y. Leow, T. A. Rahman, S. Nunoo, and S. Z. Iliya, "A comprehensive survey of pilot contamination in massive MIMO—5G system," *IEEE Commun. Surveys Tuts.*, vol. 18, no. 2, pp. 905–923, 2nd Quart., 2016.

[16] F. Wen and C. Liang, "An indoor AOA estimation algorithm for IEEE 802.11ac Wi-Fi signal using single access point," *IEEE Commun. Lett.*, vol. 18, no. 12, pp. 2197–2200, Dec. 2014.

[17] J. Jun, L. He, Y. Gu, W. Jiang, G. Kushwaha, V. A., L. Cheng, C. Liu, and T. Zhu, "Low-overhead WiFi fingerprinting," *IEEE Trans. Mobile Comput.*, vol. 17, no. 3, pp. 590–603, Mar. 2018.

[18] L. Chen, P. Thevenon, G. Seco-Granados, O. Julien, and H. Kuusniemi, "Analysis on the TOA tracking with DVB-T signals for positioning," *IEEE Trans. Broadcast.*, vol. 62, no. 4, pp. 957–961, Dec. 2016.

[19] L. Chen, O. Julien, P. Thevenon, D. Serant, A. G. Pena, and H. Kuusniemi, "TOA estimation for positioning with DVB-T signals in outdoor static tests," *IEEE Trans. Broadcast.*, vol. 61, no. 4, pp. 625–638, Dec. 2015.

[20] W. Li, P. Wei, and X. Xiao, "A robust TDOA-based location method and its performance analysis," *Sci. China F, Inf. Sci.*, vol. 52, no. 5, pp. 876–882, May 2009.

[21] S. He and S.-H.-G. Chan, "Wi-Fi fingerprint-based indoor positioning: Recent advances and comparisons," *IEEE Commun. Surveys Tuts.*, vol. 18, no. 1, pp. 466–490, 1st Quart., 2016.

[22] J. Shen, A. F. Molisch, and J. Salmi, "Accurate passive location estimation using TOA measurements," *IEEE Trans. Wireless Commun.*, vol. 11, no. 6, pp. 2182–2192, Jun. 2012.

[23] X. Li, S. Li, D. Zhang, J. Xiong, Y. Wang, and H. Mei, "Dynamic-MUSIC: Accurate device-free indoor localization," in *Proc. ACM Int. Joint Conf. Pervas. Ubiquitous Comput. (UbiComp)*, Heidelberg, Germany:, 2016, pp. 196–207.

[24] Y. Liu and H. Cui, "Antenna array signal direction of arrival estimation on digital signal processor (DSP)," *Procedia Comput. Sci.*, vol. 55, pp. 782–791, Jan. 2015.

[25] K. He, Y.-G. Chen, X. Jia, and L. Jia, "A stagewise fast DOA estimation method based on sparse signal representation," in *Proc. 12th Int. Conf. Signal Process. (ICSP)*, Hangzhou, China, Oct. 2014, pp. 1925–1929.

[26] H. Steendam and M. Moeneclaey, "Analysis and optimization of the performance of OFDM on frequency-selective time-selective fading channels," *IEEE Trans. Commun.*, vol. 47, no. 12, pp. 1811–1819, 1999.

[27] L. Grigoryan, M. Aivazyan, and A. Babayan, "MIMO OFDM DOA estimation algorithm implementation and validation using SDR platform," *J. Commun. Softw. Syst.*, vol. 15, no. 1, pp. 1–8, 2019.

[28] T. B. Lavate, V. K. Kokate, and A. M. Sapkal, "Performance analysis of MUSIC and ESPRIT DOA estimation algorithms for adaptive array smart antenna in mobile communication," in *Proc. 2nd Int. Conf. Comput. Netw. Technol.*, Bangkok, Thailand, 2010, pp. 308–311.

[29] C.-B. Ko and J.-H. Lee, "Performance of ESPRIT and root-MUSIC for angle-of-arrival (AOA) estimation," in *Proc. IEEE World Symp. Commun. Eng. (WSCE)*, Singapore, Dec. 2018, pp. 49–53.

[30] N. P. Waweru, D. B. Konditi, and P. K. Langat, "Performance analysis of MUSIC, root-MUSIC and ESPRIT DOA estimation algorithm," *World Acad. Sci., Eng. Technol., Int. J. Elect., Comput., Energetic, Electron. Commun. Eng.*, vol. 8, no. 1, pp. 209–216, 2014.

[31] M. Emadi, E. Miandji, and J. Unger, "OMP-based DOA estimation performance analysis," *Digit. Signal Process.*, vol. 79, pp. 57–65, Aug. 2018.

[32] J. Wang, S. Kwon, and B. Shim, "Generalized orthogonal matching pursuit," *IEEE Trans. Signal Process.*, vol. 60, no. 12, pp. 6202–6216, Dec. 2012.
[33] P. Vallet, X. Mestre, and P. Loubaton, "Performance analysis of an improved MUSIC DoA estimator," *IEEE Trans. Signal Process.*, vol. 63, no. 23, pp. 6407–6422, Dec. 2015.
[34] G. Z. Karabulut, T. Kurt, and A. Yongacoglu, "Angle of arrival detection by matching pursuit algorithm," in *Proc. IEEE 60th Veh. Technol. Conf. (VTC-Fall)*, Los Angeles, CA, USA, vol. 1, Sep. 2004, pp. 324–328.
[35] N.-H. Ho, P. Truong, and G.-M. Jeong, "Step-detection and adaptive step-length estimation for pedestrian dead-reckoning at various walking speeds using a smartphone," *Sensors*, vol. 16, no. 9, p. 1423, Sep. 2016.
[36] *Ettus Research*. Accessed: 2020. [Online]. Available: http://www.ettus.com/

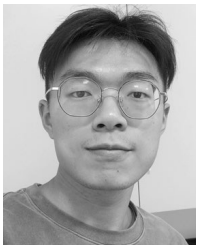

XIN ZHOU received the B.S. degree from the School of Remote Sensing and Information Engineering, Wuhan University, China, where he is currently pursuing the M.S. degree in surveying and mapping engineering. His research interests include indoor positioning and navigation technology based on signal of opportunity, wireless communications, and the Internet of Things.

LIANG CHEN was a Senior Research Scientist with the Department of Navigation and Positioning, Finnish Geodetic Institute, Finland. He is currently a Professor with the State Key Laboratory of Information Engineering in Surveying, Mapping, and Remote Sensing, Wuhan University, China. He has published over 70 scientific articles and five book chapters. His current research interests include indoor positioning, wireless positioning, sensor fusion, and location-based services. He is currently an Associate Editor of *Journal of Navigation, Navigation, and Journal of Institute of Navigation*.

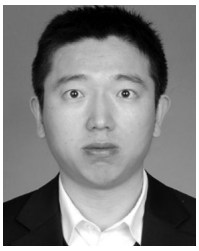

JUN YAN received the Ph.D. degree in electrical engineering from Southeast University, Nanjing, China, in 2012. He was a Visiting Scholar with the Department of Computer and Electronics Engineering, University of Nebraska–Lincoln, Lincoln, in 2014, and a Research Scientist with the Department of Electrical and Computer Engineering, Concordia University, in 2016. He is currently an Associate Professor with the College of Telecommunications and Information Engineering, Nanjing University of Posts and Telecommunications. His research interest is statistical signal processing for wireless location.

RUIZHI CHEN is currently a Professor and the Director of the State Key Laboratory of Information Engineering in Surveying, Mapping, and Remote Sensing, Wuhan University. Prior to that, he was an Endowed Chair Professor with Texas A&M University–Corpus Christi, USA, the Head and a Professor of the Department of Navigation and Positioning, Finnish Geodetic Institute, Finland, and the Engineering Manager of Nokia, Finland. He has published two books and more than 200 scientific articles. His current research interests include indoor positioning, satellite navigation, and location-based services.